

1 Article

2 Strain ratio as a quantification tool in strain imaging

3 Roald Flesland Havre^{1,2*}, Jo Erling Riise Waage³, Anesa Mulabecirovic^{2,4}, Odd Helge Gilja^{1,2,4},
4 Lars Birger Nesje^{1,2,4}

5 ¹ Department of Medicine, Haukeland University Hospital, Bergen, Norway

6 ² National Centre for Ultrasound in Gastroenterology, Department of Medicine, Haukeland University
7 Hospital, Bergen, Norway

8 ³ Nordsjællands Hospital, Department of Surgery, Hillerød, Denmark

9 ⁴ Institute of Clinical Medicine (K1), University of Bergen, Bergen Norway

10

11 * Correspondence: roald.flesland.havre@helse-bergen.no; Tel.: +47-55972872 (office) +47-90842938 (mobile)

12

13 **Featured Application:** Strain based elastography. In this paper the system used is Real-Time
14 Elastography, (Hitachi Medical Corporation, Zug, Switzerland) with relevant probes for external
15 and endoscopic applications.

16 Abstract:

17 1) Background: Ultrasound-based strain imaging is now available in several ultrasound (US)
18 scanners. Strain ratio (SR) can be used to quantify strain recorded simultaneously in two different
19 user-selected areas, ideally exposed to the same amount of stress. The aim of this study was to
20 evaluate SR variability when assessed in an in-vitro setup with a tissue-mimicking phantom, on
21 resected tissue samples and in live tissue scanning with endoscopic applications. 2) Material and
22 methods: Retrospective analysis of SR for quantification of elastic contrasts in a tissue-mimicking
23 phantom containing four homogenous inclusions, in 38 resected bowel wall lesions and in 48 focal
24 pancreatic lesions examined in vivo. Median SR and the inter-quartile range (IQR) was calculated
25 on all external and endoscopic US-applications. The IQR/median provides a measure of the SR
26 variability focusing on the two percentiles of the data closest to the median value. 3) Results: The
27 overall variability of SR was lowest in a tissue-mimicking phantom (mean QR/median SR: 0.07). In
28 resected bowel wall lesions representing adenomas, adenocarcinomas or Crohn lesions, the
29 variability increased (mean IQR/Median: 0.62). During an endoscopic examination of focal
30 pancreatic lesions in vivo, the variability increased further (mean IQR/Median: 2.04). 4) Conclusion:
31 SR variability increased when assessed on different targets with growing heterogeneity and
32 biological variability as one moved from homogeneous media to live tissues and endoscopic
33 application. This may indicate a limitation for the accuracy SR evaluation in clinical applications.

34 **Keywords:** Ultrasound, strain elastography, quantification, strain ratio, strain quantification,
35 measurement variability, pancreas, EUS, Crohn's disease, carcinoma

36

37

38

39

40

41 1. Introduction

42 Soft tissue elastic properties change in various pathological tissues such as malignant tumors
 43 and inflammatory processes. Strain elastography can be used to quantify this physical feature based
 44 on ultrasound imaging [1]. Tissue hardness can be assessed across tissue images describing the
 45 Elastic modulus (E), defined as the relationship between the application of local stress and the
 46 resulting strain. This can be expressed as:
 47

$$E = \frac{\Delta \text{strain}}{\Delta \text{stress}} \quad (1)$$

48
 49 Since the stress is not recorded as it travels from the stress source through the tissue and
 50 gradually attenuates, it is not possible to calculate the Elastic modulus from strain data alone. This
 51 phenomenon is sometimes referred to as the “inverse problem” of strain elastography [2]. Under
 52 similar stress, strain in harder tissue is lower than strain in softer tissue. Thus, a comparison between
 53 strain in reference tissue and in the lesion, produces a ratio that increases when the focal lesion is
 54 harder. SR represents the relative difference in tissue hardness and was originally introduced as
 55 the “Fat lesion ratio” [3]. The definition of SR is:
 56

$$\text{Strain Ratio (SR)} = \frac{\text{Mean strain B (reference area)}}{\text{Mean strain A (lesion area)}} \quad (2)$$

57
 58
 59 Hooke’s law states that for small deformations in elastic media the strain is linearly
 60 proportional with the force (stress) applied to it. However, this is true for isotropic, homogeneous
 61 media with near infinite or free border conditions [4]. These conditions are rarely present in
 62 biological tissues, which exhibit non-linear elastic properties of different magnitude due to
 63 differences in tissue structure and function [5, 6, 7]. This may be of importance for the accuracy of
 64 strain elastography. By keeping the pre-compression and range of compressions (Δ Stress) to a
 65 limited interval, the stress-strain relation of the tissues involved may for practical purposes be
 66 regarded as linear.

67
 68 Vital tissue contains ducts and veins acting as dampers of stress as well as connective tissue and
 69 sliding anatomical surfaces that limit and enhance tissue movement, respectively. Unintended
 70 movements may cause strain concentration and reduce accuracy in SR evaluation. Hence, in-vivo
 71 conditions often do not meet the preconditions of Hooke’s law for elasticity calculation, and may
 72 therefore represent limitations and cause strain-imaging artefacts that increases variability and
 73 probably reduce the reproducibility of SR measurements.

74 SR expresses a momentarily and relative difference in compressibility in two user selected areas
 75 within selected regions of interest in a strain elastogram. SR depends on similar stress application to
 76 the two areas compared and similar stress attenuation in the tissue between the stress source (probe)
 77 and the area of interest [8]. The SR measurement method was first introduced as the
 78 “Fat-lesion-ratio” in breast imaging, where an area of subcutaneous fat was used as reference to
 79 mean strain in the lesion under investigation [3]. Using the subcutaneous fat as reference was
 80 perhaps as close to a standardized reference tissue one can get. However, the same preconditions
 81 apply as the position and probe distance to a hard or soft lesion may influence the strain distribution
 82 in reference area fat tissue [8].
 83

84 The variations in elasticity of biological tissues is not linear with varying pre-compression or
 85 stretch of the tissue [9]. For breast and pancreatic tissues this has been evaluated by force

86 indentation and deformation studies under increasing strengths [5, 6]. This implies that the amount
87 of pre-compression and the range of the stress applied influences the strain result, and thereby the
88 elastogram. In one study, the authors recommend a pre-compression level less than 0.2-0.4 kPa in
89 breast imaging [6].
90

91 Another physical condition that complicates reproducibility of strain ratios is the temporal
92 variability of a live strain cine-loop [10]. The best phases for acquiring strain data is during the
93 compression and decompression phase, since there is no strain signal when the stress is stable
94 between these two phases. Compression and decompression of vital tissue may be caused by
95 applied pressure from the probe or by natural internal movements from arterial pulsation, heart
96 movements or even breathing. Some strain elastography platforms provide feedback to the
97 examiner about the phase of compression or decompression on which the image is acquired,
98 enabling the use of SR from similar phases of tissue straining.
99

100 The aim of this study was to retrospectively compare SR variability as expressed by the median
101 value and interquartile range (IQR) recorded in homogeneous tissue-mimicking media, in resected
102 tissue from bowel lesions and during endosonography of focal pancreatic lesions.
103

104 2. Materials and Methods

105 The SR data in this study were recorded on different versions of the Hitachi Medical
106 Corporations Real-Time Elastography (RTE) operated on HV-900 and Ascendus platforms. US data
107 were acquired using external linear probes (L54, 9-13 MHz) as well as Pentax echo endoscope
108 EG-3870 UTK (Pentax Medical, Hamburg, Germany). The phantom used is a standard model made
109 of Zerdine® embedded in a firm box including eight spherical inclusions with elasticity 8 kPa, 14
110 kPa, 45 kPa and 80 kPa in a background of 25 kPa (CIRS, model 49, NC, USA).
111

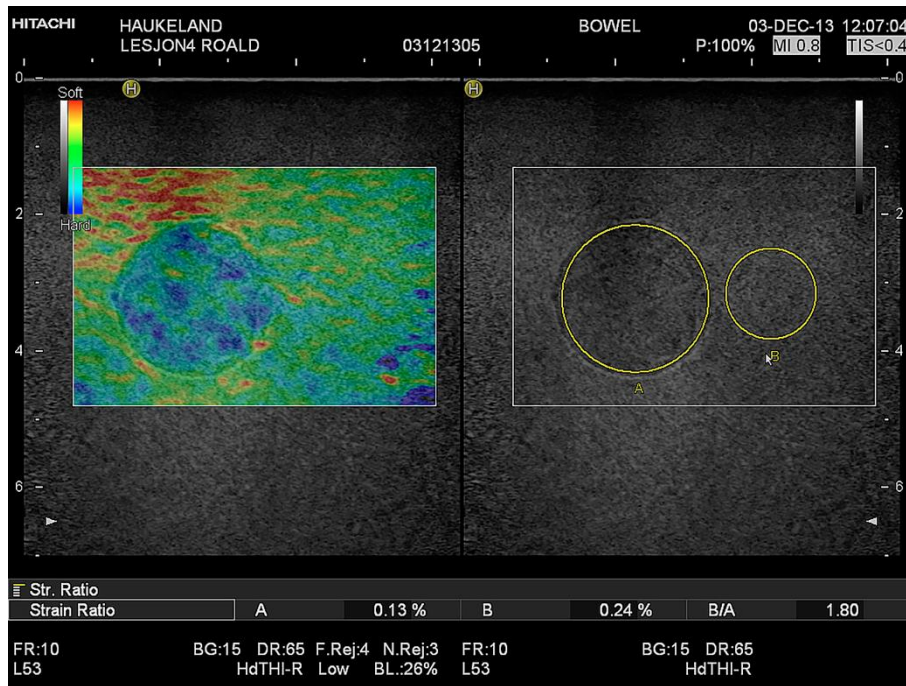
112 Statistical Methods

113 We used the mean of median SR values for each class of lesion, the range of values (max-min)
114 and the interquartile range (IQR) for different objects or lesions. The IQR is a measure of the
115 variability based on the two central quartiles from 25-75 percentile. The remaining 50% in the
116 eccentric quartiles, are not part of the IQR, but are encountered for by the range, representing the
117 gap between the highest and lowest measured value. Kolmogorov-Smirnov's test was used to
118 determine the distribution of data, and one way ANOVA or non-parametric tests were used
119 accordingly. We then used the Kruskal- Wallis test for individual samples to compare the Median
120 SR, the IQR and the IQR/Median for the three applications of Real-Time elastography with SR. We
121 also analyzed the difference for Median SR, IQR and IQR/Median between observer A and B in the
122 phantom and for benign or malignant pancreatic lesions by EUS elastography using one way
123 ANOVA and T-test. A difference with p-value <0.05 was considered statistically significant.
124

125 All patients had signed a consent form to participate in the two studies that provided SR data
126 for comparison of variability. For statistical analysis, we used SPSS, version 24 (SPSS, IBM, NY,
127 USA). Study protocols as well as patient information & consent forms were approved by the
128 institutional committee for Research in Medicine and Biology. The studies were conducted
129 according to the Helsinki Declaration for Research in Medicine and Biology.

130 3. Results

131 In a homogeneous, tissue-mimicking phantom, four spherical inclusions with elasticity different
132 from the background were examined by two different observers. Observer A had little experience
133 with US scanning and observer B had long experience with both phantom and clinical application of
134 US strain imaging methods. An image of inclusion 4 (80 kPa +/-12 kPa) is shown in Fig 1.



135

136 Fig 1: Elastogram from a tissue-mimicking phantom displaying a spherical inclusion (80kPa) with a
 137 diameter of 2 cm in a background of 25 kPa. Right side: B-mode image with area markings; A (lesion)
 138 and B (reference). Left side: elastogram in color coding. The stress source was working from above in
 139 the axial direction. The lesion is speckled, green-blue while the background material is mostly
 140 homogeneously green. Between the lesion and the probe the red color indicates strain concentration
 141 between the stress source and the harder lesion. The Strain ratio is Mean strain in B / Mean strain in
 142 A = 1.80.

143 In Table 1 the median values of ten repeated SR measurements are reported for observer A and B,
 144 their range and interquartile range (IQR) and the IQR/median. The last measure represents the
 145 variability of 50% of the central observations divided by the median value. The common mean value
 146 for observer A and B was 0.07. IQR for all median SR values for all inclusions was ≤ 0.17 .

147

148

149

150

151

152

153

154

155

156

157

158
159
160

Table 1. Elastography strain ratio in four inclusions in a tissue-mimicking phantom

Lesion	1		2		3		4	
	8 kPa		14 kPa		45 kPa		80 kPa	
Observer	A	B	A	B	A	B	A	B
Median SR	0.52	0.68	0.96	0.82	1.91	1.35	2.50	2.82
Range	0.09	0.08	1.04	0.10	0.18	0.11	0.91	0.24
IQR ¹ 25-75	0.06	0.03	0.15	0.06	0.12	0.04	0.17	0.07
IQR/Median	0.118	0.044	0.156	0.073	0.063	0.030	0.068	0.025

161 ¹IQR: Inter Quartile Range. Mean IQR/median for phantom lesions: 0.07

162

163 Interobserver variability

164 The interobserver variability in the phantom lesions expressed by the mean of SR medians
165 showed no significant difference for the two observers ($p=0.937$ ANOVA). The IQR/Median SR
166 ranged from 0.063-0.156 (Mean: 0.101) for observer A with least experience, and 0.025-0.073 (Mean
167 0.043) for observer B with more experience, but the difference was not significant ($p=0.055$ ANOVA).

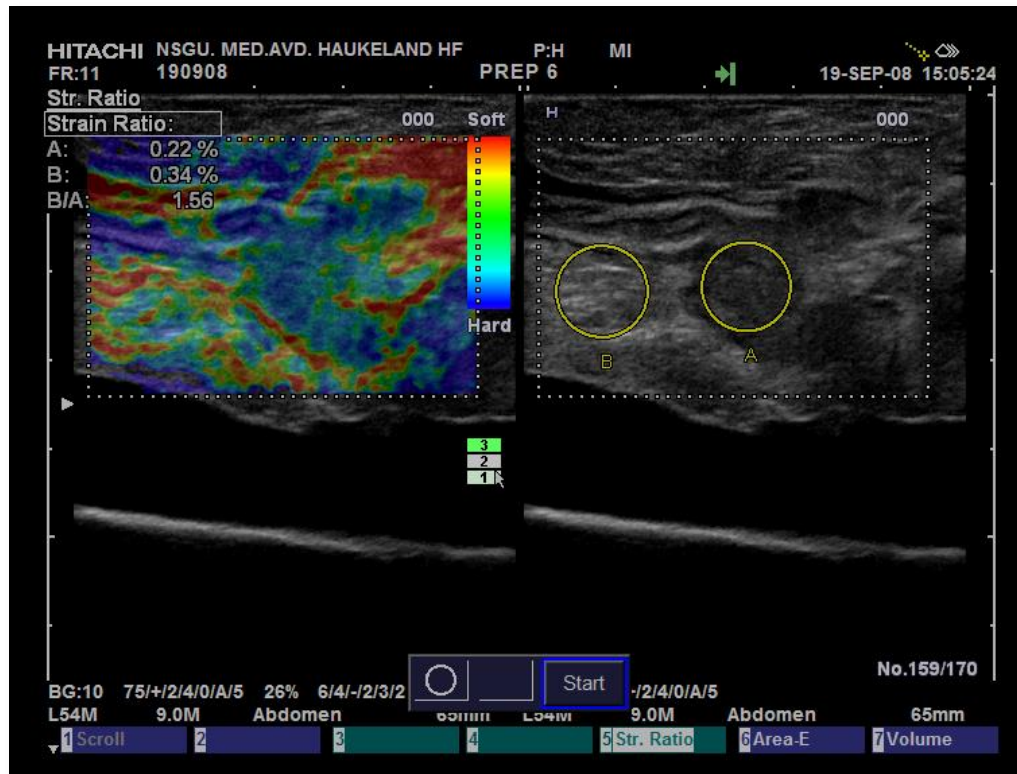
168 The distributions of Median SR and IQR/median were not significantly different between
169 observer A and B. The mean IQR alone was significantly different between observer A: 0.125
170 (SD:0.050) and observer B 0.050 (SD:0.018) ($p=0.027$ ANOVA). Range was not significantly different
171 between the observers.

172

173 Strain ratio in surgical specimens

174 One observer scanned surgically removed bowel specimens including tumors or resected
175 Crohn lesions. The image of a scanned bowel wall with an adenocarcinoma is shown in Fig 2. SR was
176 recorded between normal bowel wall and peri-colic fat/ connective tissue and the lesion of interest.
177 SR results including range, IQR and IQR/median for the entities adenoma, Crohn lesions and
178 adenocarcinomas are reported in Table 2. Crohn lesions had a very wide range in measurements
179 (21.44), but this entity had the lowest IQR/Median: 0.31. For adenocarcinomas, the IQR/Median was
180 0.66 and for adenomas, represented by a very limited number (4), the IQR/Median was 0.88. For all
181 SR measurement in resected bowel tissue the variability expressed by IQR was ≤ 0.88 . The mean
182 IQR/Mean in all resected tissue was 0.62.

183



184
185 Fig 2: Elastogram of a newly resected bowel lesion from the colon containing a malignant tumor
186 (adenocarcinoma). The hypoechoic tumor mass (right) is imaged with a blue-green color indicating harder
187 tissue (left). A strain ratio measured between pericolic fat and connective tissue as well as part of the proper
188 muscle and the tumor tissue yields SR=1.56. The lesion and reference are positioned at similar depth and
189 distance from the stress source and the bottom.

190
191
192

Table 2. Elastography Strain ratio in resected surgical bowel specimens

	Adenoma	Crohn	Adenocarcinoma
Number	4	16	18
Median SR	1.25	2.09	2.18
Range	1.38	21.44	4.53
IQR ¹ (25-75)	1.10	0.64	1.44
IQR/Median	0.88	0.31	0.66

193 ¹IQR: Inter Quartile Range. Mean IQR/Median for ex vivo tissue: 0.62

194

195 Strain ratios in live tissue using endosonography

196 The data on pancreatic lesions representing various focal entities is reported in Table 3. The mean and range of
197 these data has previously been published [11]. The mean of Median SR of malignant pancreatic lesions was
198 7.05 (SD 1.85) and for the benign lesions it was 2.15 (SD 1.22), (p=0.035 T-test). For all entities, the IQR was

199 higher than the median value of SR, indicating substantial variability. For the malignant lesions the mean
 200 IQR/Median SR was 1.79 (SD 0.69). For the benign lesions the mean IQR/Median SR was 2.21 (SD 1.29). The
 201 difference was not significant ($p=0.713$, T-test). The mean IQR/Median SR for all pancreatic focal lesions were
 202 2.04. The IQR/Median SR value for lesions in focal pancreatitis was the highest value for all lesions, reflecting
 203 the large variability observed in focal pancreatitis as well as a relatively low Median SR for this entity (0.91).

204

205 **Table 3.** Elastography strain ratio of focal pancreatic lesions by Endoscopic Ultrasound

206

Entity	NET undetermined or benign	NET malignant	Adenocarcin oma	Focal pancreatitis	Other benign lesion
Number	11	7	11	8	11
Median SR	2.19	5.74	8.36	0.91	3.34
Range	7.93	17.5	24.5	8.33	35.3
IQR ¹ (25-75)	2.80	13.1	10.9	3.55	5.53
IQR/Median	1.28	2.28	1.30	3.68	1.66

207 ¹IQR: Inter Quartile Range. Mean IQR/Median for pancreatic lesions: 2.04

208

209 IQR/Median SR for three applications of strain elastography

210 For the three applications reported here the IQR/median SR increased from scanning a tissue
 211 mimicking phantom to ex-vivo surgical specimens of bowel pathology and further when the strain
 212 imaging was performed endoscopically focusing on focal pancreatic lesions. The difference between
 213 the IQR/Median SR was significant ($p=0.002$, Kruskal-Wallis) Fig. 3.

214

215

216

217

218

219

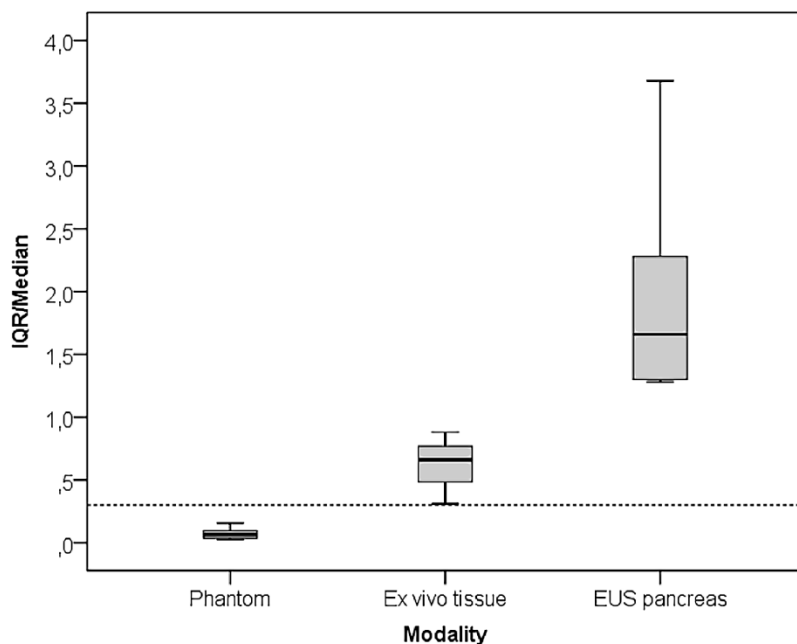
220

221

222

223

224



225

226 Fig. 3: Box plots of the IQR/Median SR for the different applications of strain based elastography (Real-Time
 227 Elastography) reported here. There is significant difference between this quality parameter for the three
 228 applications ($p=0.002$). In liver elastography using Transient Elastography, the suggested maximum
 229 IQR/Median for good quality assessment in 10 repeated measurements in the same liver is 0.30, which is
 230 marked with the dotted horizontal line.

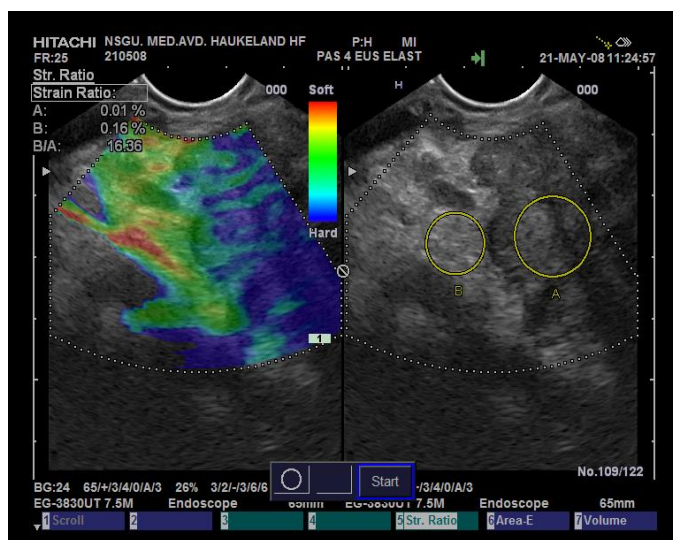
231

232 Reference area variability

233 Fig. 4 demonstrates three different frames (A-C) of strain images by EUS elastography
 234 including SR measurements of the same pancreatic tumor using slightly different, but relevant
 235 reference areas. The three SRs obtained range from 8.43 – 16.36 – 25.70. All the variation is caused by
 236 variability in the reference tissue, in which strain varies between 0.08% - 0.16% - 0.27%. The lesion
 237 strain was 0.01% in all images.

238

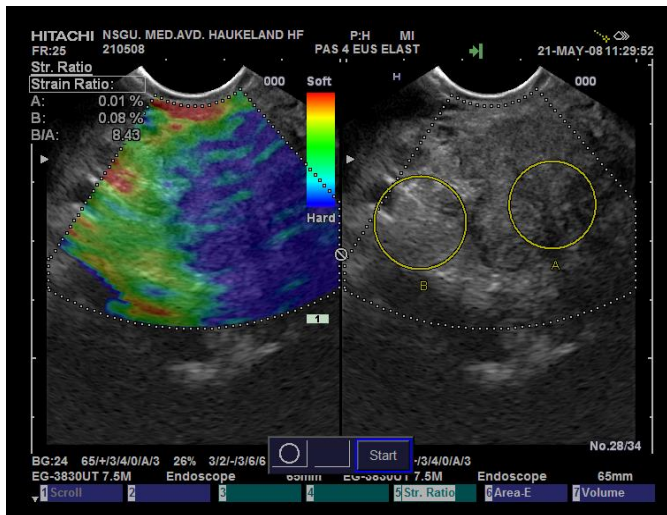
239



240

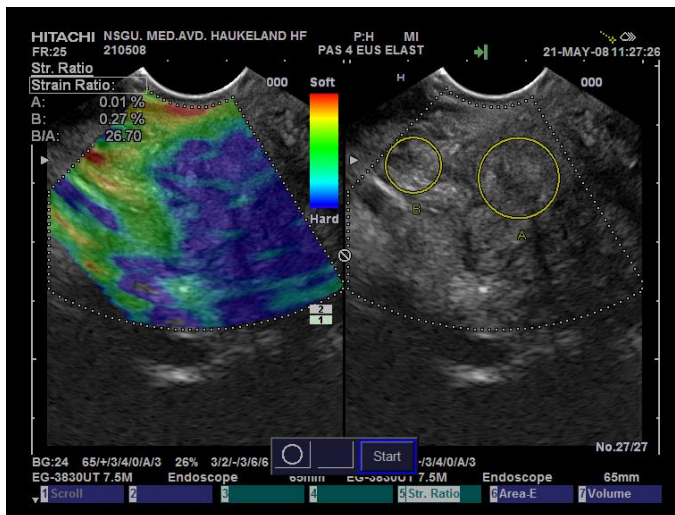
241

A



242
243
244

B



245
246
247

C

248 *Fig. 4: Three images of the same pancreatic tumor visualized by EUS elastography. Tumor tissue is blue in the*
 249 *elastograms with a predominantly green reference tissue. The position and size of the reference tissue vary*
 250 *slightly between the three different images, and exhibit different strains in all three images, A: 0.16% B: 0.08%*
 251 *and C: 0.27%, while the strain in the lesion remains 0.01%. This causes the SR values to vary from 8.43-26.7.*

252 4. Discussion

253 In this paper, we have presented SR measurement in a tissue-mimicking phantom and in
 254 resected tissue where the stress is applied by pushing gently with the probe itself focusing on the
 255 measurement variability. We have also presented data from endosonography of focal pancreatic
 256 lesions where arterial pulsations, particularly from the aorta, acts as an internal stress source. We
 257 have shown that the IQR increases with complexity and anisotropy in the tissues to a level that
 258 surpasses the median value of SR. The mean value in of the IQR/Median increases 8,6 times from
 259 phantom (0.07) to resected tissue (0.62) and 28,3 times to endosonographic application (2.04).

260
 261 Selection of the reference area for comparison with a focal lesion also introduce variability
 262 which may influence the equation and the resulting SR more than the strain variability of the lesion
 263 itself. (Fig 4). Some researchers have only recorded the strain value in the lesion of interest, and
 264 found that it performs equally well as the strain ratio in some applications [12, 13]. This however, is
 265 dependent on a near standardized application of stress to the lesions of interest. But usually the
 266 amount of stress cannot be sufficiently standardized, and depends on type of application, lesion and

267 patient related factors such a depth of lesion and elasticity of surrounding tissue. For the endoscopic
268 application, also the pulse pressure, the aortic compliance and the presence of peri-pancreatic soft
269 tissue would be different from patient to patient. Therefore, a standardization of the stress applied to
270 the lesion of interest in endoscopic strain elastography is almost impossible to establish. Moreover,
271 further differences may be caused by variable levels of pre-compression and applied stress. Since
272 soft tissues have non-linear elastic properties, the tissue will appear harder with more applied stress
273 or increased pre-compression [5] [6]. On the other hand, this strain-stress profile under different
274 levels of stress may be a valuable signature of the different soft tissue, including pathological lesions,
275 and may be used for tissue characterization if a series of graded stress pulses may be applied to the
276 ROI.

277 Another way to quantify a strain image is by making a strain histogram [14]. This shows the
278 distribution of the different colors representing different strain intervals in a 256 scale, from no strain
279 (0) to max strain as set by the scanner software (256). From a histogram it is also possible to quantify
280 the distribution of recorded strains to evaluate if the lesion and reference tissue is homogeneous or
281 heterogeneous by using kurtosis and range. The median value of the histogram represents the
282 median hardness of the lesion. Some researchers have suggested to use median histogram value of
283 reference tissue divided by the median value of the lesion histogram to create a "histogram ratio". In
284 a study of pancreatic lesions, this did not perform better than SR with a ROC-AUC of 0.843 and a
285 cut-off selection yielding a specificity of 98%, and a sensitivity of only 50%. (accuracy of 69%) [15].

286 Visual evaluation of the elastogram is direct and intuitive and requires no post-processing.
287 Several scoring systems for categorical scoring of strain images have been proposed. For breast
288 imaging the 5-point Tsukuba scale was proposed by Itoh et al. in 2006 [16] . Amended versions of
289 this visual score have been proposed for other organs, e.g. the pancreas and lymph nodes by EUS
290 elastography [17]. Both continuous VAS score and categorical visual scores for endoscopic
291 assessment of rectal tumors has shown comparable results with SR measurements [18]. In a
292 comparative study of SR and the 5-point visual elastography breast scale, SR came out with better
293 accuracy [19]. The direct visual impression the experienced examiner gets by elastography imaging,
294 however, may contain more information than a 5-step visual score can comprehend, and is useful in
295 many cases for lesions in doubt. With training, different aspects of the elastogram such as strain
296 concentration and artefacts caused by veins and natural sliding surfaces can be recognized. These
297 findings can hardly be recognized by SR, histograms or other formal quantification methods. One
298 group has investigated the use of automated pattern- and color recognition of elastography of focal
299 pancreatic lesions in 258 patients. They used an artificial neural network image- analysis and
300 information about the histological diagnosis from endoscopic elastography as input. This improved
301 the accuracy by ROC-AUC to 0.94, significantly better compared to using only lesion strain
302 histograms that had a ROC-AUC of 0.85. This evaluation was done from material in a multicenter
303 study [20] but required substantial post-processing.

304 Using an endoscopic application in live tissue, the stress is mainly caused by arterial pulsations,
305 heartbeat or breathing. An endoscopic application is also challenging because the probe is inserted
306 into the gastrointestinal cavity, and cannot be controlled directly by the observer's hands, in the
307 same manner as in external strain imaging ultrasonography. Lu and Chen et al. performed a
308 meta-analysis of EUS elastography in pancreatic lesions evaluated qualitatively by a visual score, by
309 strain histograms, SR, contrast enhanced EUS and EUS FNA [21]. They identified a large range in
310 SR cut-off values based on previous published cut-off values or the ROC curves (3.05 to 24.82). This
311 was reason to large heterogeneity for the specificity, and 3/8 studies were identified as outliers. After
312 removing the outliers, the evaluation for identification of malignant lesions based on qualitative
313 visual scores and strain histograms outperformed the SR based evaluation (sens: 0.94, spes: 0.54,
314 Diagnostic OR: 29.42, Q: 0.812). On the other hand, strain elastography and SR based assessment of
315 rectal tumors using a dedicated radial rectal probe has been used to improve selection of patients for
316 organ-sparing treatment compared to standard multidisciplinary assessment [22].

317
318

319 **Limitations:**

320 This study is based on previously recorded strain ratios from a tissue mimicking phantom and
321 real tissues both in-vitro and in-vivo. The data is based on different numbers of lesions for each
322 application. For the resected tissue and the EUS-elastography of pancreatic focal lesions, all
323 recordings are done by the same observer, while the phantom inclusions are done by two observers.
324 The fact that the data on surgical specimens and pancreatic lesions in this study are collected from
325 individual lesions and patients while the phantom inclusions represent only four different “cases”
326 also serves to limit the variability in the phantom SR measurements. The same strain elastography
327 system was used for all scans (Real-Time elastography, RTE), but both scanners and software were
328 upgraded between the first and the last recording.

329

330 **Recommendations for measuring SR in soft tissues**

331 Based on our experience with strain elastography in-vitro and in-vivo we propose the following
332 advice to obtain relevant and reproducible elastograms:

333

- 334 • Select a US-plane where the lesion can be compared with relevant reference tissue, where
335 both may be exposed to similar stress.
- 336 • Reference area should be applied to relevant tissue and be of similar size if possible. A too
337 small reference area may cause sampling error.
- 338 • Select lesion and reference tissue at approximately same distance from the stress source if
339 possible. In external imaging, the stress source is most often equivalent with the probe.
- 340 • Avoid sliding anatomical surfaces and visible vessels or ducts as part of the reference area.
- 341 • Measure SR in the same phase of compression or decompression when several
342 measurements are being recorded.
- 343 • Measure at least three repeated SR – use the median

344

345 **5. Conclusions**

346 SR measurements are useful for quantifying local differences in tissue strain. We have shown
347 that SR as a semi-quantitative method, has increased variability when targeted on a tissue
348 mimicking phantom, resected biological tissue and vital tissue examined by endoscopic
349 ultrasonography, respectively. Target area characteristics may limit the method’s accuracy in clinical
350 applications. SR also depends on similar stress application in reference and lesion areas.
351 Homogeneous tissue facilitates SR measurements. Soft lesions have low SR values and relatively low
352 variability, while harder lesions have higher SR measurement and variability. Attenuation of stress
353 with depth and tissue inhomogeneity and anisotropy increase strain variability.

354

355 **Acknowledgments:** The studies that are reported data from in this paper are all conceived at Department of
356 Medicine and the National Centre for Ultrasound in Gastroenterology (NCGU), Haukeland University
357 Hospital. The funding of equipment and salaries were provided by the Medical Department, Haukeland
358 University Hospital and University of Bergen, Institute of clinical Medicine. The studies were supported by
359 MedViz an interdisciplinary research cluster from Haukeland University Hospital, University of Bergen and
360 Christian Michelsen Research AS. We thank professor emeritus Svein Ødegaard for his tutoring and guidance
361 and specialist nurse Eva Fosse for her great support during data acquisition. We will also express our gratitude
362 to the support and guidance we have been given from the application specialists in Hitachi Medical
363 Corporation, Europe. Hitachi Medical Corporation has not provided equipment for free nor has had any
364 influence on the planning, execution or reporting in the studies reported.

365

366

367

368 **Author Contributions:** Havre, R.F. and Nesje, L.B. and Gilja O.H. planned the studies and provided the
369 equipment. Nesje L.B. and Gilja O.H. supervised in the collection of data, analyses and writing of the
370 manuscript. Havre R.F. collected and analyzed the data and wrote the manuscript. Waage J.E.R. was a
371 consultant in performing the elastography study on surgical specimens and pancreatic lesions with Real-Time
372 Elastography. He also prepared the manuscript. Mulabecirovic A. presented preliminary data at DDW 2016
373 and prepared the manuscript.

374 **Conflicts of Interest:** The authors declare no conflict of interest. The founding sponsors had no role in the
375 design of the study; in the collection, analyses, or interpretation of data; in the writing of the manuscript, and in
376 the decision to publish the results.

377 Appendix A

378 S1: Excel file containing data based on the median SR for different phantom inclusions and
379 etiologies (see it in the supplementary file)

380

381 References

- 382 1. Ophir, J.; Cespedes, I.; Ponnekanti, H.; Yazdi, Y.; Li, X., Elastography: a quantitative method for
383 imaging the elasticity of biological tissues. *Ultrason Imaging* **1991**, 13, (2), 111-34.
- 384 2. Aghajani, A.; Haghapanhi, M.; Nikazad, T., The ultrasound elastography inverse problem and the
385 effective criteria. *Proc Inst Mech Eng H* **2013**, 11, (227), 1203-12.
- 386 3. Ueno, E.; Umemoto, T.; Bando, H.; Tohno, E.; Waki, K.; Matsumura, T., New Quantitative method in
387 Breast elastography: Fat lesion ratio (FLR). In *Radiological Society of North America Scientific Assembly and*
388 *Annual Meeting*, Chicago, Illinois, USA, 2007.
- 389 4. Diamond, L.; Murphy, M. Lesson: Stress, Strain and Hooke's Law.
390 [https://www.teachengineering.org/view_lesson.php?url=collection/van_/lessons/van_cancer_lesson2/](https://www.teachengineering.org/view_lesson.php?url=collection/van_/lessons/van_cancer_lesson2/van_cancer_lesson2.xml)
391 [van_cancer_lesson2.xml](https://www.teachengineering.org/view_lesson.php?url=collection/van_/lessons/van_cancer_lesson2/van_cancer_lesson2.xml) (April 11 2018),
- 392 5. Krouskop, T. A.; Wheeler, T. M.; Kallel, F.; Garra, B. S.; Hall, T., Elastic moduli of breast and prostate
393 tissues under compression. *Ultrason Imaging* **1998**, 20, (4), 260-74.
- 394 6. Umemoto, T.; Ueno, E.; Matsumura, T.; Yamakawa, M.; Bando, H.; Mitake, T.; Shiina, T., Ex vivo and
395 in vivo assessment of the non-linearity of elasticity properties of breast tissues for quantitative strain
396 elastography. *Ultrasound Med Biol* **2014**, 40, (8), 1755-68.
- 397 7. Ponnekanti, H.; Ophir, J.; Huang, Y.; Cespedes, I., Fundamental mechanical limitations on the
398 visualization of elasticity contrast in elastography. *Ultrasound Med Biol* **1995**, 21, (4), 533-43.
- 399 8. Havre, R. F.; Waage, J. R.; Gilja, O. H.; Odegaard, S.; Nesje, L. B., Real-Time Elastography: Strain Ratio
400 Measurements Are Influenced by the Position of the Reference Area. *Ultraschall Med* **2011**, 33, (6), 10.
- 401 9. Le Sant, G.; Ates, F.; Brasseur, J. L.; Nordez, A., Elastography Study of Hamstring Behaviors during
402 Passive Stretching. *PLoS One* **2015**, 10, (9), e0139272.
- 403 10. Bamber, J.; Cosgrove, D.; Dietrich, C. F.; Fromageau, J.; Bojunga, J.; Calliada, F.; Cantisani, V.; Correas,
404 J. M.; D'Onofrio, M.; Drakonaki, E. E.; Fink, M.; Friedrich-Rust, M.; Gilja, O. H.; Havre, R. F.; Jenssen,
405 C.; Klausner, A. S.; Ohlinger, R.; Saftoiu, A.; Schaefer, F.; Sporea, I.; Piscaglia, F., EFSUMB guidelines
406 and recommendations on the clinical use of ultrasound elastography. Part 1: Basic principles and
407 technology. *Ultraschall Med* **2013**, 34, (2), 169-84.
- 408 11. Havre, R. F.; Odegaard, S.; Gilja, O. H.; Nesje, L. B., Characterization of solid focal pancreatic lesions
409 using endoscopic ultrasonography with real-time elastography. *Scand J Gastroenterol* **2014**, 49, (6),
410 742-51.

- 411 12. Iglesias-Garcia, J.; Larino-Noia, J.; Abdulkader, I.; Forteza, J.; Dominguez-Munoz, J. E., Quantitative
412 endoscopic ultrasound elastography: an accurate method for the differentiation of solid pancreatic
413 masses. *Gastroenterology* **2010**, *139*, (4), 1172-80.
- 414 13. Dawwas, M. F.; Taha, H.; Leeds, J. S.; Nayar, M. K.; Oppong, K. W., Diagnostic accuracy of quantitative
415 EUS elastography for discriminating malignant from benign solid pancreatic masses: a prospective,
416 single-center study. *Gastrointest Endosc* **2012**, *76*, (5), 953-61.
- 417 14. Riishede, I.; Ewertsen, C.; Carlsen, J.; Petersen, M. M.; Jensen, F.; Nielsen, M. B., Strain Elastography for
418 Prediction of Malignancy in Soft Tissue Tumours--Preliminary Results. *Ultraschall Med* **2015**, *36*, (4),
419 369-74.
- 420 15. Opacic, D.; Rustemovic, N.; Kalauz, M.; Markos, P.; Ostojic, Z.; Majerovic, M.; Ledinsky, I.; Visnjic, A.;
421 Krzrnaric, J.; Opacic, M., Endoscopic ultrasound elastography strain histograms in the evaluation of
422 patients with pancreatic masses. *World J Gastroenterol* **2015**, *21*, (13), 4014-9.
- 423 16. Itoh, A.; Ueno, E.; Tohno, E.; Kamma, H.; Takahashi, H.; Shiina, T.; Yamakawa, M.; Matsumura, T.,
424 Breast disease: clinical application of US elastography for diagnosis. *Radiology* **2006**, *239*, (2), 341-50.
- 425 17. Giovannini, M.; Thomas, B.; Erwan, B.; Christian, P.; Fabrice, C.; Benjamin, E.; Genevieve, M.; Paolo,
426 A.; Pierre, D.; Robert, Y.; Walter, S.; Hanz, S.; Carl, S.; Christoph, D.; Pierre, E.; Jean-Luc, V. L.; Jacques,
427 D.; Peter, V.; Andrian, S., Endoscopic ultrasound elastography for evaluation of lymph nodes and
428 pancreatic masses: a multicenter study. *World J Gastroenterol* **2009**, *15*, (13), 1587-93.
- 429 18. Waage, J. E.; Rafaelsen, S. R.; Borley, N. R.; Havre, R. F.; Gubberud, E. T.; Leh, S.; Kolbro, T.; Hagen, K.
430 K.; Eide, G. E.; Pfeffer, F., Strain Elastography Evaluation of Rectal Tumors: Inter- and Intraobserver
431 Reproducibility. *Ultraschall Med* **2015**.
- 432 19. Zhi, H.; Xiao, X. Y.; Yang, H. Y.; Ou, B.; Wen, Y. L.; Luo, B. M., Ultrasonic elastography in breast cancer
433 diagnosis: strain ratio vs 5-point scale. *Acad Radiol* **2010**, *17*, (10), 1227-33.
- 434 20. Saftoiu, A.; Vilmann, P.; Gorunescu, F.; Janssen, J.; Hocke, M.; Larsen, M.; Iglesias-Garcia, J.;
435 Arcidiacono, P.; Will, U.; Giovannini, M.; Dietrich, C. F.; Havre, R.; Gheorghe, C.; McKay, C.; Gheonea,
436 D. I.; Ciurea, T.; European, E. U. S. E. M. S. G., Efficacy of an artificial neural network-based approach
437 to endoscopic ultrasound elastography in diagnosis of focal pancreatic masses. *Clin Gastroenterol*
438 *Hepatol* **2012**, *10*, (1), 84-90 e1.
- 439 21. Lu, Y.; Chen, L.; Li, C.; Chen, H.; Chen, J., Diagnostic utility of endoscopic
440 ultrasonography-elastography in the evaluation of solid pancreatic masses: a meta-analysis and
441 systematic review. *Med Ultrason* **2017**, *19*, (2), 150-158.
- 442 22. Waage, J. E.; Leh, S.; Rosler, C.; Pfeffer, F.; Bach, S. P.; Havre, R. F.; Haldorsen, I. S.; Odegaard, S.;
443 Baatrup, G., Endorectal ultrasonography, strain elastography and MRI differentiation of rectal
444 adenomas and adenocarcinomas. *Colorectal Dis* **2015**, *17*, (2), 124-31.